Axisymmetric Impulsive Loading of Shallow Spherical Shells

R. PALANINATHAN* AND V. X. KUNUKKASSERIL†
Indian Institute of Technology, Madras, India

Axisymmetric forced response of shallow spherical shells is considered on the basis of an improved theory which takes into account rotatory inertia and shear deformation effects. Explicit solutions are obtained for distributed, ring and concentrated impulsive loadings with half sine, triangular, blast and rectangular pulse shapes. Natural frequencies are presented for the first 18 modes of four shell models with clamped and supported edges. Numerical results for the forced response of the shells are presented to illustrate the difference between improved and classical theories and effects of edge conditions, loading conditions, pulse shapes and pulse duration.

Nomenclature

a = base radius of the shell
S = $\bar{S}/a$, rise
h = $\bar{h}/a$, thickness
r = $\bar{r}/a$, radial coordinate
R = $(S+1/S)/2$, radius of curvature
γ = $\bar{\gamma}/a$, outer radius of loaded region
b = $\bar{b}/a$, inner radius of loaded region, radius of concentrated ring load
u, w = $(\bar{u}, \bar{w})/a$, meridional, normal displacement components
β = rotation
U_n, W_n, β_{rn} = nth normal modes of deformation components
T_1, T_2, T_3 = $\dfrac{(1-\nu^2)a}{E\bar{h}}\left[\bar{T}_1, \dfrac{12}{\bar{h}^2}\bar{T}_2, \dfrac{12}{\bar{h}^2}\bar{T}_3\right]$, spring constants
t = $\bar{t}\left[\dfrac{E}{\rho a^2(1-\nu^2)}\right]$, time
T = $\bar{T}\left[\dfrac{E}{\rho a^2(1-\nu^2)}\right]$, pulse duration
ω = $\bar{\omega}\left[\dfrac{\rho a^2(1-\nu^2)}{E}\right]$, frequency
p_r, p_n, m = $\dfrac{a(1-\nu^2)}{E\bar{h}}(\bar{p}_r, \bar{p}_n, \dfrac{12}{h^2}\bar{m})$, applied distributed forces
M_n = generalized mass corresponding to nth mode
q_n = generalized coordinate corresponding to nth mode
k_1, k_2 = $1+(1/12)(h/R)^2$, tracers which identify longitudinal and transverse inertia forces, respectively
k_r = $1+(3/20)(h/R)^2$, tracer which identifies rotatory inertia
k_s = 1.2, shear constant
ν = 0.285, Poisson ratio
E = Young's modulus
ρ = mass density
∇^2 = $(d^2/dr^2)+(1/r)(d/dr)$
$(\ ),r$ = differentiation w.r.t. radial coordinate (r)
$(\bar{\ })$ = dimensional quantities

Introduction

VARIOUS aspects concerning free vibration of shallow spherical shells are amply illustrated in Refs. 1–12. However, the research works published on the forced motion of shallow spherical shells are not to that extent. The paper by Reismann and Culkowski[13] seems to be the first systematic treatment on the axisymmetric forced motion of shallow spherical shells. However their analytical development and numerical results were restricted to distributed loading of clamped shells with Heaviside step function for the time variation of force. In a recent work,[14] the present authors have discussed axisymmetric impact loading of shallow spherical shells and the numerical results were compared with experiment. From this comparison it was possible to observe that for relatively thin shells ($\bar{h}/a \leq 0.02$) the effects of rotatory inertia and shear deformation were negligible and the results on the basis of classical theory were quite satisfactory for predicting the structural response.

Having gained confidence on the theoretical developments from the experimental studies reported in Ref. 14, it is now thought to be appropriate to conduct a detailed theoretical study on the behavior of shallow shells under various dynamic loading conditions. So, in the present paper, on the basis of classical and improved theories,[8,10] the natural frequencies and the solutions to the impulsive response of the shells are obtained for various pulse shapes, external loadings and shell parameters. Numerical results are presented extensively for the two extreme edge conditions, namely, clamped and supported edges.

Received January 24, 1973; revision received June 20, 1973.
Index category: Structural Dynamic Analysis.
* Research Scholar.
† Assistant Professor.

Solutions to Impulsive Motion

The displacement equations of motion of shallow spherical shells can be written in the form[8,13,15]

$$u_{,rr}+(u_{,r}/r)-(u/r^2)+[(1+\nu)/R]w_{,r} = k_1\ddot{u}-p_r \tag{1a}$$

$$\frac{1}{K}\left[\nabla^2 w+\beta_{,r}+\frac{\beta}{r}\right]-\frac{1+\nu}{R}\left[u_{,r}+\frac{u}{r}+\frac{2w}{R}\right] = k_2\ddot{w}-p_n \tag{1b}$$

$$-\frac{w_{,r}}{K}+\frac{h^2}{12}\left[\beta_{,rr}+\frac{\beta_{,r}}{r}-\frac{\beta}{r^2}\right]-\frac{\beta}{K} = \frac{h^2}{12}k_r\ddot{\beta}-m \tag{1c}$$

where comma and dot denote differentiation with respect to nondimensional radial coordinate and time, respectively, and $K = 2k_s/(1-\nu)$. The solution to the aforementioned system of equations can be taken in the form

$$u = \sum_{n=1}^{\infty} U_n q_n(t) \tag{2a}$$

$$w = \sum_{n=1}^{\infty} W_n q_n(t) \tag{2b}$$

$$\beta = \sum_{n=1}^{\infty} \beta_{rn} q_n(t) \tag{2c}$$

where $q_n(t)$ are the generalized coordinates and U_n, W_n, and β_{rn} are the characteristic shape functions. The shape functions U_n, W_n, and β_{rn} can be obtained by the method discussed by Kalnins.[4,10] The orthogonality of the normal modes can also be proved by the usual process.[11,15] According to the improved theory, the orthogonality conditions for a shell with elastic constraints such as shown in Fig. 1 can be easily proved to be

$$\int_0^{2\pi}\int_0^1\left(U_i U_j + W_i W_j + \frac{h^2}{12}k_r \beta_{ri}\beta_{rj}\right) r\,dr\,d\theta = 0 \quad \text{for} \quad i \neq j$$
$$= M_i \quad \text{for} \quad i = j \tag{3}$$

The term containing k_r will be absent for the case of classical theory. Substitution of Eqs. (2) into Eqs. (1) and making use of orthogonality conditions (3) will lead to the set of equations

$$\ddot{q}_n(t) + \omega_n^{\,2} q_n(t) = \frac{\int_0^{2\pi}\int_b^{\gamma} (U_n \cdot p_r + W_n \cdot p_n + \beta_{rn} \cdot m)\bar{r}\,d\bar{r}\,d\theta}{M_n} \tag{4}$$

for the determination of $q_n(t)$. In the above equations it is assumed that the shell is loaded over an annular band between the radii b and γ as shown in Fig. 1. For a shell which is at rest initially, the solution to Eq. (4) is

$$q_n(t) = \frac{P_n(r)}{\omega_n M_n}\int_0^t F_1(t')\sin\omega_n(t-t')\,dt' \tag{5a}$$

where $F_1(t')$ depends on the pulse shapes and

$$P_{n(r)} = \left[\int_0^{2\pi}\int_b (U_n p_r + W_n p_n + \beta_{rn}\cdot m)\bar{r}\,d\bar{r}\,d\theta\right]\frac{1}{M_n \omega_n} \tag{5b}$$

Now the preceding integral assumes the following values depending on the types of loading. For central concentrated normal load

$$P_n = \frac{(1-\nu^2)\bar{p}_n W(0)}{E\bar{h}aM_n\omega_n} \tag{6a}$$

For concentrated ring load at radius $\bar{b}$

$$P_n = \frac{(1-\nu^2)\bar{p}_n \cdot 2\pi\bar{b}W(b)}{E\bar{h}aM_n\omega_n} \tag{6b}$$

and for uniformly distributed load around the apex

$$P_n = \frac{(1-\nu^2)\bar{p}_n 2\pi a}{E\bar{h}M_n\omega_n}\int_0^{\gamma} W(r) r\,dr \tag{6c}$$

Now the explicit forms of the generalized coordinates given by Eq. (5a) for various interesting pulse shapes, $F_1(t)$ shown in Fig. 6 are summarised below.

1) Half sine pulse

$$q_n(t) = \frac{P_n}{[(\pi/T)^2 - \omega_n^{\,2}]}\left[\frac{\pi}{T}\sin\omega_n t - \omega_n \sin\frac{\pi}{t}t\right], \text{ for } t \leqq T \tag{7a}$$

$$q_n(t) = \frac{P_n}{[(\pi/T)^2 - \omega_n^{\,2}]}\frac{\pi}{T}[\sin\omega_n T \cdot \cos\omega_n(t-T) +$$
$$(1+\cos\omega_n T)\sin\omega_n(t-T)], \text{ for } t > T \tag{7b}$$

2) Triangular pulse

$$q_n(t) = (2P_n/\omega_n T)[t - (1/\omega_n)\sin\omega_n t], \text{ for } t \leqq T/2 \tag{7c}$$

$$q_n(t) = \frac{2P_n}{\omega_n T}\left[(T-t) - \frac{\sin\omega_n T/2}{\omega_n}\cos\omega_n(t-T/2) + (1/\omega_n)\times\right.$$
$$\left.(2-\cos\omega_n T/2)\sin\omega_n(t-T/2)\right]$$
$$\text{for } T/2 < t \leqq T \tag{7d}$$

$$q_n(t) = (2P_n/\omega_n^{\,2}T)[2(1-\cos\omega_n T/2)\sin\omega_n T/2\cos\omega_n(t-T) +$$
$$(2\cos\omega_n T/2 - (1+\cos\omega_n T))\sin\omega_n(t-T)]$$
$$\text{for } t < T \tag{7e}$$

3) Blast pulse

$$q_n(t) = (P_n/\omega_n)\{[(T-t)/T] - \cos\omega_n t + \sin\omega_n t/T\omega_n\} \text{ for } t \leqq T \tag{7f}$$

$$q_n(t) = P_n/\omega_n)\{[\cos\omega_n T/T\omega_n + \sin\omega_n T - 1/\omega_n T]\sin\omega_n \times$$
$$(t-T) + [\sin\omega_n T/T\omega_n - \cos\omega_n T]\cos\omega_n(t-T)\}$$
$$\text{for } t > T \tag{7g}$$

4) Rectangular pulse

$$q_n(t) = (P_n/\omega_n)(1-\cos\omega_n t) \quad \text{for} \quad t \leqq T \tag{7h}$$

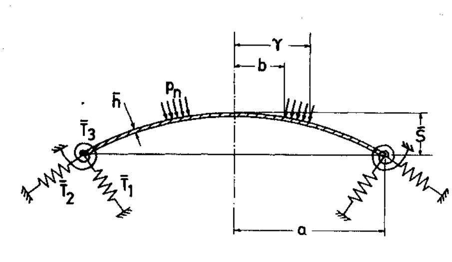

Fig. 1 Shell cross section with elastic constraints and loading.

$$q_n(t) = (P_n/\omega_n)[(1-\cos\omega_n T)\cos\omega_n(t-T) +$$
$$\sin\omega_n T\sin\omega_n(t-T)], \quad \text{for} \quad t > T \tag{7i}$$

Now the impulsive response given by Eq. (2) is completely determined for any of the loadings given by Eqs. (6) and for any one of pulse shapes given by Eqs. (7).

Numerical Results

The shell parameters used in the calculations are those of the two shell models discussed in Ref. 14 and for a thicker shell

Table 1 Natural frequencies of clamped shallow spherical shells

	Frequency parameter, ω			
	$h = 0.02$		$h = 0.04$	
Mode no.	Classical	Improved	Classical	Improved
s = 0.1444				
1	0.3273	0.3269	0.3826	0.3817
2	0.4255	0.4251	0.5615	0.5563
3	0.5947	0.5913	1.0684	1.0390
4	0.9558	0.9443	1.8470	1.7590
5	1.4524	1.4250	2.8639	2.6627
6	2.0707	2.0152	[a]3.8447	3.7172
7	2.8062	2.7063	4.1167	[a]3.8525
8	3.6561	3.4911	5.5932	4.9150
9	[a]3.8494	[a]3.8481	[a]7.0229	6.2180
10	4.6250	4.3667	7.3025	[a]7.0241
11	5.7058	5.3227	9.2371	7.6167
12	6.8996	6.3558	[a]10.1796	9.0922
13	[a]7.0261	[a]7.0243	11.4020	[a]10.1792
14	8.2111	7.4615	[a]13.3280	10.6344
15	9.6347	8.6322	13.7949	12.2295
16	[a]10.1798	9.8639	16.4121	[a]13.3282
17	11.1730	[a]10.1800	[a]16.4776	13.8703
18	12.8244	11.1527	19.2635	15.5473
19	13.3356	12.4923	[a]19.6196	[a]16.4744
s = 0.240				
1	0.4730	0.4725	0.5525	0.5501
2	0.6129	0.6112	0.7205	0.7170
3	0.7328	0.7307	1.1300	1.1022
4	1.0214	1.0107	1.8788	1.7922
5	1.4933	1.4664	2.8825	2.6826
6	2.0984	2.0435	[a]3.8650	3.7244
7	2.8259	2.7266	4.1342	[a]3.8836
8	3.6685	3.5053	5.6024	4.9260
9	[a]3.8769	[a]3.8738	[a]7.0343	6.2254
10	4.6376	4.3802	7.3117	[a]7.6376
11	5.7153	5.3329	9.2419	7.6238
12	6.9050	6.3638	[a]10.1895	9.0971
13	7.0424	[a]7.0380	11.4060	[a]10.1882
14	8.2177	7.4692	[a]13.3348	10.6393
15	9.6397	8.6382	13.7986	12.2328
16	[a]10.1898	9.8684	16.4103	[a]13.3352
17	11.1777	[a]10.1903	[a]16.4878	13.8737
18	12.8283	11.1573	19.2644	15.5497
19	[a]13.3364	12.4961	[a]19.6256	[a]16.4803

[a] Longitudinal mode frequency.

Table 2 Natural frequencies of supported shallow spherical shells

	Frequency parameter, ω			
	$h = 0.02$		$h = 0.04$	
Mode no.	Classical	Improved	Classical	Improved
$s = 0.1444$				
1	0.3113	0.3110	0.3804	0.3795
2	0.4240	0.4236	0.4799	0.4778
3	0.5209	0.5190	0.9013	0.8842
4	0.8453	0.8377	1.6198	1.5608
5	1.3116	1.2917	2.5791	2.4317
6	1.9005	1.8581	3.7662	3.4667
7	2.6072	2.5277	[a]3.8532	[a]3.8487
8	3.4296	3.2937	5.1934	4.6446
9	[a]3.8485	[a]3.8480	6.8427	5.9399
10	4.3683	4.1515	[a]7.0261	[a]7.0241
11	5.4205	5.0927	8.7233	7.3367
12	6.5872	6.1134	[a]10.1797	8.8169
13	[a]7.0249	[a]7.0242	10.8310	[a]10.1791
14	7.8688	7.2085	13.1654	10.3666
15	9.2639	8.3706	[a]13.3296	11.9711
16	[a]10.1798	9.5962	15.7300	[a]13.3282
17	10.7736	[a]10.1802	[a]16.4748	13.6247
18	12.3969	10.8801	18.5218	15.3159
$s = 0.240$				
1	0.4582	0.4579	0.5259	0.5241
2	0.5901	0.5885	0.6975	0.6960
3	0.7107	0.7099	0.9717	0.9556
4	0.9173	0.9102	1.6553	1.5971
5	1.3558	1.3363	2.6001	2.4537
6	1.9304	1.8885	3.7745	3.4803
7	2.6286	2.5496	[a]3.8848	[a]3.8755
8	3.4451	3.3099	5.2034	4.6559
9	[a]3.8749	[a]3.8737	6.8478	5.9479
10	4.3815	4.1655	[a]7.0424	[a]7.0376
11	5.4306	5.1032	8.7285	7.3441
12	6.5950	6.1218	[a]10.1895	8.8209
13	[a]7.0396	[a]7.0378	10.8354	[a]10.1878
14	7.8756	7.2166	13.1670	10.3709
15	9.2695	8.3768	[a]13.3388	11.9745
16	[a]10.1897	9.6012	15.7320	[a]13.3352
17	10.7785	[a]10.1898	[a]16.4815	13.6281
18	12.4009	10.8846	18.5233	15.3183

[a] Longitudinal mode frequency.

with $\bar{h}/a = 0.04$. Extensive calculations were necessary to determine the natural frequencies, amplitude ratios, generalized mass, and the summation of infinite series to obtain the transient response. It was absolutely necessary to resort to a digital computer for the computation work and IBM 7044/1401 has been used for this purpose.

Natural frequencies for the first eighteen modes were computed for the two extreme cases of the elastic constraint (see Fig. 1) such as clamped and supported edge conditions and the results are shown in Tables 1 and 2. For a clamped edge $\bar{T}_1$, $\bar{T}_2$, and $\bar{T}_3$ shown in Fig. 1 should be considered as infinity and for a supported edge $\bar{T}_1$ and $\bar{T}_2$ should again be infinity and $\bar{T}_3$ should be set equal to zero. The values for classical theories are obtained by omitting terms containing the tracers k_r and k_s; and for improved theory by setting $k_r = 1 + 3/20 \cdot (h/R)^2$ and $k_s = 1.2$ in Eq. (1). It may be seen that the differences between the two theories are negligible for first few modes and for the 18th frequency they are of the order of 15% for $h = 0.02$ and 40% for $h = 0.04$ with respect to improved theory values, for clamped edge condition and $S = 0.1444$. The corresponding differences for supported edge conditions are 14% and 36%. Similarly the differences between clamped and supported edge conditions are negligible at lower frequencies and they are of the order of 4% and 1.6% at 18th frequency, respectively, for classical and improved theories ($S = 0.1444$, $h = 0.04$).

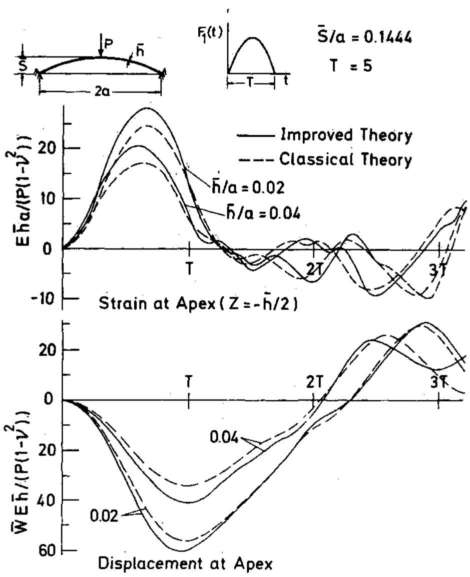

Fig. 2 Effect of thickness on the deformation of clamped shallow spherical shells.

The results for the impulsive response under various loading conditions are presented in Figs. 2–7. Since the peak deflections and strains produced by the improved theory are seen to be slightly higher than that predicted by classical theory, to be on a conservative side it is considered to be advisable to present all the results on the basis of improved theory except in Fig. 2 where the difference between the two theories are illustrated for two thickness to radius ratios. The results shown in these figures are meant to illustrate the following aspects; 1) the difference between the results based on improved and classical theories, 2) influence of edge conditions, 3) effect of the types of external loadings, 4) influence of pulse shapes and 5) effect of pulse duration.

From Fig. 2 it is seen that the difference on the strain between the two theories is about 14% for $h = 0.02$ and 17% for $h = 0.04$. The respective differences on deflections are 7% and 20%. The extent of the influence of the edge conditions on deformation may be seen from Figs. 3 and 4. The difference in the strain at the apex between clamped and supported edges, as seen from Fig. 3, is almost negligible, except for some time lag in the free part. From Fig. 4, it is seen that the apex deflection is the same during the period of loading regardless of the edge and loading conditions.

The effects of the types of loading on deformation are illustrated in Figs. 4 and 5. From Fig. 4, it is evident that the apex deflections are not very much affected by the different

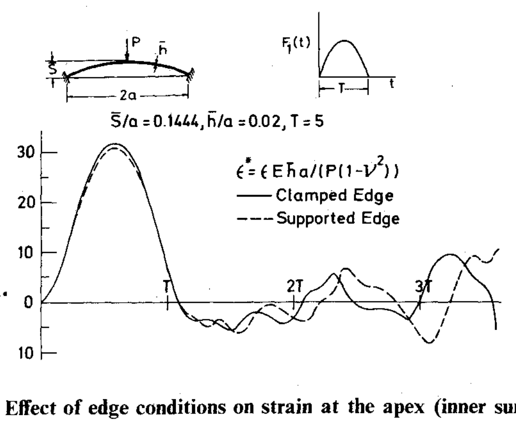

Fig. 3 Effect of edge conditions on strain at the apex (inner surface).

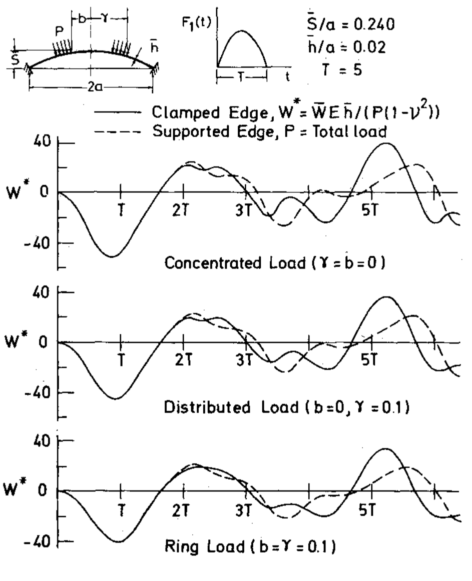

Fig. 4 Effect of the types of loadings and support conditions on the apex deflection.

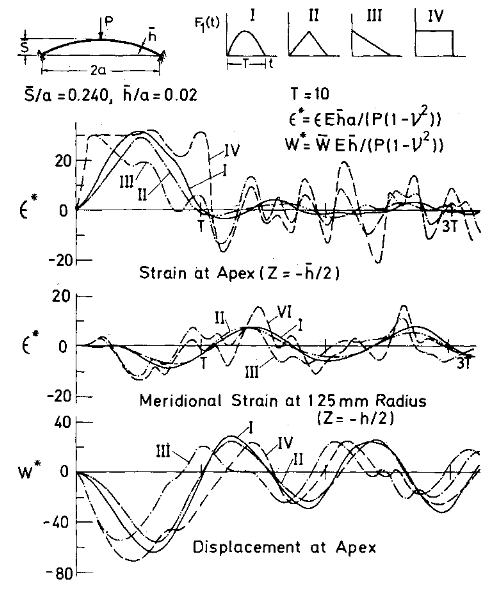

Fig. 6 Effect of pulse shapes on the deformation of clamped shallow spherical shells.

types of loads. However, from Fig. 5 it is clear that there is considerable effect on the magnitudes of strains. From this figure it may be seen that with respect to the bending strain the magnitude of direct strain at the apex is about 25% for concentrated load and 55% for ring load.

The influence of pulse shapes is shown in Fig. 6. It is interesting to note from this figure that the variation of strains at the apex are of similar shapes as that of the forcing pulses considered. However, it is not so for the strains at 125 mm radius and for the deflections at the apex. The magnitudes of the peak strains produced at the apex by the different pulse shapes are almost the same but the deflections produced are somewhat different. Rectangular pulse is seen to be producing the maximum peak deflection while the blast pulse (curve III) develops the minimum deflection among the four shapes considered.

The effect of pulse duration on deformation is illustrated by Fig. 7. It may be seen from Fig. 7 that the shorter pulse produces more number of circles of zero normal deflection than the longer ones. This illustrates the reason for the need of more number of terms to achieve a specified degree of convergence in the series summation for transient response computation.

Conclusions

In this paper results are presented for the two extreme edge conditions, namely, clamped and supported edges. However, the natural frequencies and dynamic deformation can be obtained for intermediate (constrained) edge conditions, by substituting the appropriate values of spring constants in nondimensional form in the frequency determinants. In a previous report,[14] the authors have checked the validity of the numerical results by conducting experiments on shell models with thickness to radius ratio of 0.02. From these experimental results it was observed that for relatively thin shells ($\bar{h}/a \leq 0.02$) it will be sufficient to use classical theory to obtain satisfactory estimation of the dynamic behavior. So, it is now assumed that the shallow shell

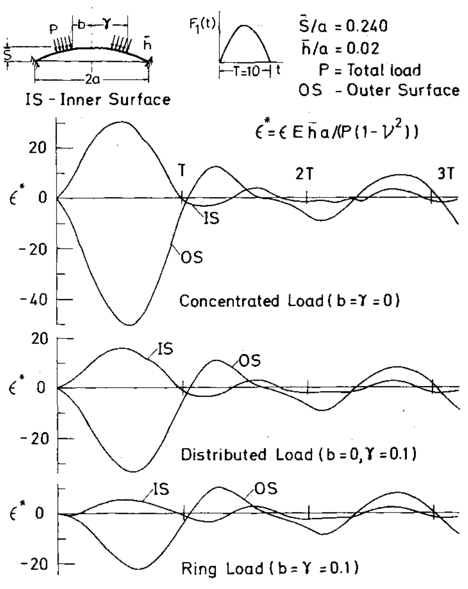

Fig. 5 Effect of the types of loadings on the apex strains for clamped edge.

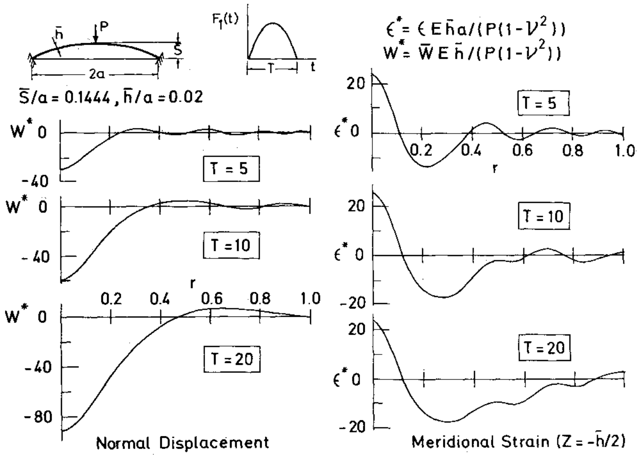

Fig. 7 Effect of pulse duration on deformation across a radial section at the peak load ($t = T/2$).

theories and results presented in this paper can be more confidently used for design purposes.

References

[1] Federhofer, K., "Zur Berechnung der Eigenchingungen der Kugelschale," *Akademie der Wissenchaften in Wien, Sitzungsberichte, Mathematik-Naturwissenschaft, Klasse,* Vol. 146, No. 2A, 1937, pp. 57–69.

[2] Reissner, E., "On Vibrations of Shallow Spherical Shells," *Journal of Applied Physics,* Vol. 17, Dec. 1946, pp. 1038–1042.

[3] Reissner, E., "On Axisymmetric Vibrations of Shallow Spherical Shells," *Quarterly of Applied Mathematics,* Vol. 13, No. 3, Oct. 1955, pp. 279–290.

[4] Kalnins, A. and Naghdi, P. M., "Axisymmetric Vibrations of Shallow Elastic Spherical Shells," *Journal of the Acoustical Society of America,* Vol. 32, No. 3, March 1960, pp. 342–347.

[5] Hoppmann, W. H., II, "Frequencies of Vibration of Shallow Elastic Spherical Shells," *Journal of Applied Mechanics,* Vol. 28, Ser. E, No. 2, June 1961, pp. 305–307.

[6] Kalnins, A., "Free Nonsymmetric Vibrations of Shallow Spherical Shells," *Proceedings of 4th U.S. National Congress of Applied Mechanics,* Vol. 1, 1962, pp. 225–233.

[7] Hoppmann, W. H., II and Baronet, C. N., "A Study of the Vibrations of Shallow Spherical Shells," *Journal of Applied Mechanics,* Vol. 30, No. 3, Sept. 1963, pp. 329–334.

[8] Koplik, B. and Yu, Y. Y., "Axisymmetric Vibrations of Homogeneous and Sandwich Spherical Caps," *Journal of Applied Mechanics,* Vol. 34, No. 3, Sept. 1967, pp. 667–673.

[9] Kunukkasseril, V. X. and Palaninathan, R., "Free Vibrations of Shallow Spherical Shells," Rept. AM/E 15, Dept. of Applied Mechanics, Indian Inst. of Technology, Madras, India.

[10] Kalnins, A., "On Vibrations of Shallow Spherical Shells," *Journal of the Acoustical Society of America,* Vol. 33, 1961, pp. 1102–1107.

[11] Kalnins, A., "Vibration and Stability of Prestressed Shells," *Nuclear Engineering and Design,* Vol. 20, 1972, pp. 131–147.

[12] Kraus, H. and Kalnins, A., "Transient Vibration of Thin Elastic Shells," *Journal of the Acoustical Society of America,* Vol. 38, 1965, pp. 994–1002.

[13] Reismann, H. and Culkowski, P. M., "Forced Axisymmetric Motion of Shallow Spherical Shells," *Journal of the Engineering Mechanics Division, ASCE,* Vol. 94, No. EM 2, April 1968, pp. 653–670.

[14] Kunukkasseril, V. X. and Palaninathan, R., "Concentrated Impact Loading of Shallow Spherical Shells," Rept. AM/E 21, Dept. of Applied Mechanics, Indian Inst. of Technology, Madras, India.

[15] Kraus, H., *Thin Elastic Shells,* Wiley, New York, 1967, pp. 363–366.